Molecular Systems
Design & Engineering

PAPER

View Article Online
View Journal | View Issue

Cite this: *Mol. Syst. Des. Eng.*, 2018, **3**, 66

Evaluation of circularly polarized luminescence in a chiral lanthanide ensemble†

Yoshinori Okayasu[a] and Junpei Yuasa *[ab]

This work demonstrates a methodology for the evaluation of circularly polarized luminescence of a chiral europium(III) (Eu^{III}) complex species in an ensemble system. The chiral Eu^{III} complex species consists of chiral bis(oxazolinyl)pyridine [(*R*)- or (*S*)-iPr-Pybox] and β-diketonate ligands with a pendant nitro group (DK-NO_2). The pendant NO_2 group in [iPr-Pybox](Eu^{III})(DK-NO_2)$_3$ (monometallic Eu^{III} species) coordinates to the Eu^{III} center of another Eu^{III} complex, giving rise to the generation of a chiral Eu^{III} ensemble consisting of mono-, di-, and the other oligomeric Eu^{III} species, $\{$[iPr-Pybox](Eu^{III})(DK-NO_2)$_3\}_n$. The luminescence dissymmetry factors (g_{lum}) of the chiral Eu^{III} ensemble have been successfully determined by using a commercially available fluorescence spectrophotometer attached with a rotatable $\lambda/4$ filter and a fixed linearly polarized plate. This study suggests that the chiral Eu^{III} ensemble in solution displays a large circularly polarized luminescence ($|g_{lum}|$ = 0.19) as compared to that of a reference monometallic complex [iPr-Pybox](Eu^{III})(DK-CN)$_3$ ($|g_{lum}|$ = 0.11–13). The larger g_{lum} is primarily attributed to the contribution of the dimetallic Eu^{III} species exhibiting a high degree of circular polarization in luminescence (g_{lum2} = 0.27) in the ensemble. Conversely, a large linearly polarized component was observed in luminescence from the chiral Eu^{III} ensemble in the solid state (KBr pellet).

Received 30th August 2017,
Accepted 20th September 2017

DOI: 10.1039/c7me00082k

rsc.li/molecular-engineering

Design, System, Application

This work demonstrated the quantitative evaluation of circularly polarized luminescence in a chiral europium(III) (Eu^{III}) ensemble consisting of several Eu^{III} complex species. Circularly polarized luminescence (CPL) has become one of the hottest research topics in photochemistry due to its intriguing photonic applications, including circularly polarized electroluminescence (CPEL) for 3D displays, quantum information processing and optical data storage. Typically, chiral lanthanide complexes are promising circularly polarized luminescence materials in view of obtaining a high degree of circular polarization in luminescence because of their remarkable emission features of magnetically-allowed intraconfigurational f–f transitions. In this context, the recent rapid development of supramolecular lanthanide chemistry has provided us new opportunities for the evaluation of circularly polarized luminescence in an ensemble consisting of several chiral lanthanide complex species, where each complex exhibits different chiroptical properties. This work describes how to evaluate the luminescence dissymmetry factor of the chiral Eu^{III} ensemble. The present work would expand the scope of the design of molecules and systems with intriguing chiroptical properties.

Introduction

Circularly polarized luminescence (CPL) has become one of the hottest research topics in photochemistry. The main reason may be due to its intriguing photonic applications, including circularly polarized electroluminescence (CPEL) for 3D displays, quantum information processing and optical data storage.[1–3] Typically, chiral lanthanide complexes are promising circularly polarized luminescence materials in view of obtaining a high degree of circular polarization in luminescence because of their remarkable emission features of magnetically-allowed intraconfigurational f–f transitions.[4–11] The magnetic dipole transition satisfies the magnetic-dipole selection rule, $\Delta J = 0, \pm 1$ (except $0 \leftrightarrow 0$), thus often exhibiting extremely large circular polarization in luminescence.[12,13] In this context, the recent rapid development of supramolecular lanthanide chemistry[14–18] has provided us new opportunities for the evaluation of circularly polarized luminescence in an ensemble consisting of several chiral lanthanide complex species, where each complex exhibits different chiroptical properties (*e.g.*, luminescence dissymmetry factor). Thus, a simple evaluation methodology for circularly polarized luminescence of a chiral lanthanide ensemble would expand the scope of supramolecular chiral lanthanide systems.

In the present work, we demonstrate the evaluation of circularly polarized luminescence in a chiral europium(III) (Eu^{III})

---

[a] *Department of Applied Chemistry, Tokyo University of Science, 1-3 Kagurazaka, Shinjuku, Tokyo 162-8601, Japan. E-mail: yuasaj@rs.tus.ac.jp*

[b] *A Precursory Research for Embryonic Science and Technology (PRESTO), Science and Technology Agency (JST), 4-1-8 Honcho, Kawaguchi, Saitama 332-0012, Japan*

† Electronic supplementary information (ESI) available. See DOI: 10.1039/c7me00082k

ensemble consisting of several Eu^{III} complex species (Fig. 1).[19] The chiral Eu^{III} complex species consists of chiral bis(oxazolinyl) pyridine [(*R*)- or (*S*)-iPr-Pybox] and β-diketonate ligands acting as antennas for generating Eu^{III} luminescence. The β-diketonate ligand ($DK\text{-}NO_2$) contains a pendant nitro group which serves as a second coordination site for the Eu^{III} center.[20] The chiral Eu^{III} complex ([(*R*)- or (*S*)-iPr-Pybox](Eu^{III})($DK\text{-}NO_2$)$_3$) was employed as a simple cross-linked complex to afford the chiral lanthanide ensemble systems. The monometallic Eu^{III} species spontaneously self-associates in solution conditions, giving rise to the generation of a chiral Eu^{III} ensemble consisting of mono-, di-, and the other oligomeric Eu^{III} species, {[(*R*)- or (*S*)-iPr-Pybox](Eu^{III})($DK\text{-}NO_2$)$_3$}$_n$. We have chosen the ligand pair (iPr-Pybox and $DK\text{-}NO_2$) based on our previous work, where tris[β-diketonate (1,1,1,5,5,5-hexafluoropentane-2,4-dione)] Eu^{III} complexes containing the chiral iPr-Pybox ligand exhibited strong circularly polarized luminescence with good emission efficiency.[21] The present work revealed that the chiral Eu^{III} ensemble displays a strong circularly polarized luminescence ($|g_{lum}| = 0.19$) mainly due to the contribution of the dimetallic chiral Eu^{III} species with a large luminescence dissymmetry factor ($|g_{lum2}| = 0.27$) in the chiral ensemble.

Experimental

General

Chemicals were purchased from Wako Pure Chemical Industries Ltd. and used as received without further purification. (*R*,*R*)- and (*S*,*S*)-2,6-bis(4-isopropyl-2-oxazolin-2-yl)pyridine were obtained from Tokyo Chemical Industry Co., Ltd. (TCI). 4,4,4-Trifluoro-1-(4-nitrophenyl)butane-1,3-dione and 4,4,4-trifluoro-1-(4-cyanophenyl)butane-1,3-dione ($DK\text{-}NO_2$ and DK-CN, respectively) were prepared according to the procedure described previously.[22] The emission lifetimes were recorded using a FluoroCube (HORIBA, 3000 U-YSP). The positive ESI mass spectra of the chiral Eu^{III} complexes were measured with mass spectrometers (JEOL AccuTOF CS JMS-T100CS for ESI). The emission and UV-vis absorption spectra were measured at room temperature using JASCO FP-6500 and V-660, respectively.

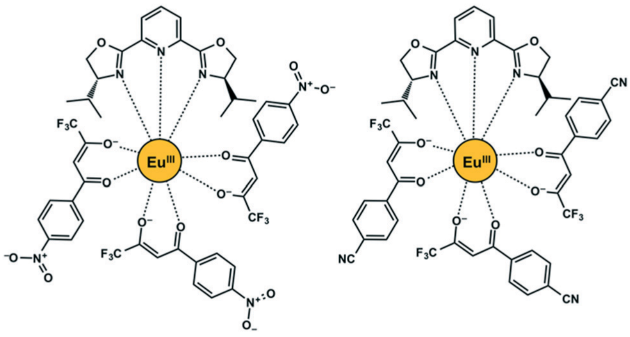

[(*R*)-*i*Pr-Pybox](Eu^{III})($DK\text{-}NO_2$)$_3$ **[(*R*)-*i*Pr-Pybox](Eu^{III})(DK-CN)$_3$**

Fig. 1 Chemical structures of [(*R*)-iPr-Pybox](Eu^{III})($DK\text{-}NO_2$)$_3$ and [(*R*)-iPr-Pybox](Eu^{III})(DK-CN)$_3$.

Synthesis of [iPr-Pybox](Eu^{III})($DK\text{-}NO_2$)$_3$ and [iPr-Pybox](Eu^{III})(DK-CN)$_3$

Precursor complexes, [(Eu^{III})($DK\text{-}NO_2$)$_3$(H_2O)$_2$] and [(Eu^{III})(DK-CN)$_3$(H_2O)$_2$], were prepared as described in the literature.[23] Typically, [(*R*)-iPr-Pybox](Eu^{III})($DK\text{-}NO_2$)$_3$ was synthesized as follows. (*R*,*R*)-2,6-bis(4-isopropyl-2-oxazolin-2-yl)pyridine (0.17 mmol) and [(Eu^{III})($DK\text{-}NO_2$)$_3$(H_2O)$_2$] (0.17 mmol) were dissolved in methanol (30 mL) in a reaction flask. The reaction mixture was stirred overnight at room temperature. After removing the solvent by evaporation, the obtained white powder was washed with distilled water and dried under vacuum (yield: 73%). HRMS [ESI-MS (positive)]: the monometallic complex, *m*/*z* calcd. for $C_{47}H_{38}EuF_9N_6O_{14}Na^+$ [[iPr-Pybox](Eu^{III})($DK\text{-}NO_2$)$_3$ + Na]$^+$, 1257.14122; found 1257.14024, the dimetallic complex: *m*/*z* calcd. for $C_{94}H_{76}Eu_2F_{18}N_{12}O_{28}Na^+$ [{[iPr-Pybox](Eu^{III})($DK\text{-}NO_2$)$_3$}$_2$ + Na]$^+$ 2491.30147, found 2491.29268. [(*S*)-iPr-Pybox](Eu^{III})($DK\text{-}NO_2$)$_3$ and reference chiral Eu^{III} complexes, [(*R*)- or (*S*)-iPr-Pybox](Eu^{III})(DK-CN)$_3$ were prepared using the same procedures as those for [(*R*)-iPr-Pybox](Eu^{III})($DK\text{-}NO_2$)$_3$. HRMS [ESI-MS (positive)]: *m*/*z* calcd. for $C_{50}H_{38}EuF_9N_6O_8Na^+$ [[iPr-Pybox](Eu^{III})(DK-CN)$_3$ + Na]$^+$ 1197.17174, found 1197.16884.

Determination of the luminescence dissymmetry factor

The luminescence dissymmetry factor (g_{lum}) of the chiral Eu^{III} complexes was determined using the experimental setup designed based on a fluorescence spectrofluorometer (JASCO FP-6500) with a rotatable $\lambda/4$ filter and a fixed linearly polarized plate (Fig. 5).[14a] The emission was corrected after passing through the rotatable $\lambda/4$ filter and the fixed linearly polarized plate every two degrees of the angle (θ) between the rotatable $\lambda/4$ filter and the fixed linearly polarized plate. The observed emission intensity (I_{obs}) periodically decreases and increases in response to the angle (θ) [Fig. 6a and b], wherein the intensity at the angle $\theta = 45$, 225 and that at 135, 315 degrees correspond to the right- and left-CPL intensity, respectively (I_R and I_L, respectively) from the sample. The g_{lum} values were calculated by using the equation, $g_{lum} = 2(I_L - I_R)/(I_L + I_R)$. The system precision is checked by using a standard material, a cesium tetrakis(3-heptafluoro-butylryl-(+)-camphorato) Eu^{III} complex, $Cs^+[Eu((+)\text{-}hfbc)_4]^-$. The determined g_{lum} value (1.41) is close to the literature value ($g_{lum} = 1.38$).[13] These details are further outlined in the text (*vide infra*).

Results and discussion

Chiral Eu^{III} ensemble

Chiral Eu^{III} complexes with the general formula [(*R*)- or (*S*)-iPr-Pybox](Eu^{III})($DK\text{-}NO_2$)$_3$ were synthesized by reacting the tris($DK\text{-}NO_2$) Eu^{III} complex [(Eu^{III})($DK\text{-}NO_2$)$_3$(H_2O)$_2$] with (*R*)- or (*S*)-iPr-Pybox in a 1 : 1 stoichiometry in methanol. Interestingly, the resulting chiral Eu^{III} complex displays a non-single-exponential emission decay in acetonitrile solution (Fig. 2a, $\lambda_{em} = 618$ nm due to the $^5D_0 \rightarrow {}^7F_2$ transition of Eu^{III}).[14] The

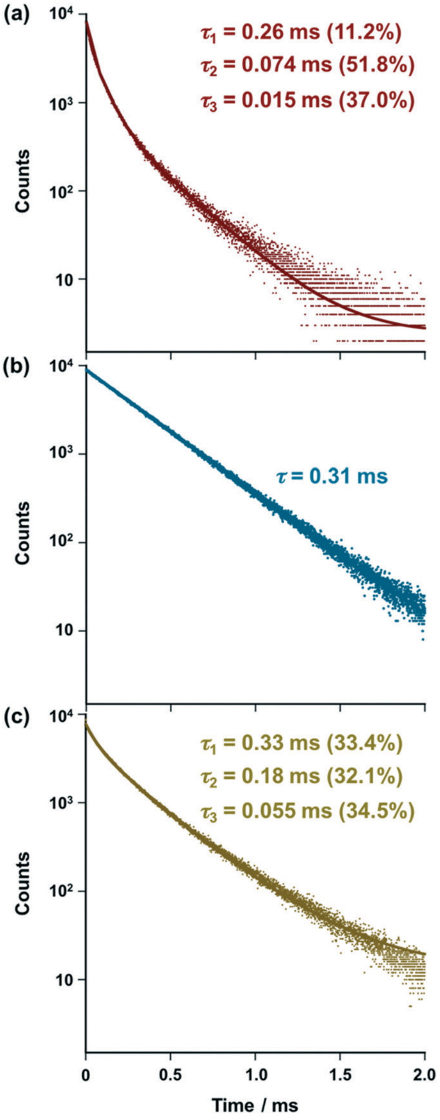

Fig. 2 Emission decay curves at 618 nm of (a) [(*R*)-iPr-Pybox](Eu^{III})(DK-NO$_2$)$_3$ and (b) [(*R*)-iPr-Pybox](Eu^{III})(DK-CN)$_3$ in acetonitrile at 298 K (concentration: 1.0 × 10^{-5} M), and (c) that of [(*R*)-iPr-Pybox](Eu^{III})(DK-NO$_2$)$_3$ in the solid state (KBr pellet). Excitation-wavelength: λ_{ex} = 347 nm. The solid lines show (a) and (c) multi-exponential curve fitting [$I(t) = A_1\exp(-t/\tau_1) + A_2\exp(-t/\tau_2) + A_3\exp(-t/\tau_3)$] and (b) single-exponential curve fitting [$I(t) = A\exp(-t/\tau)$].

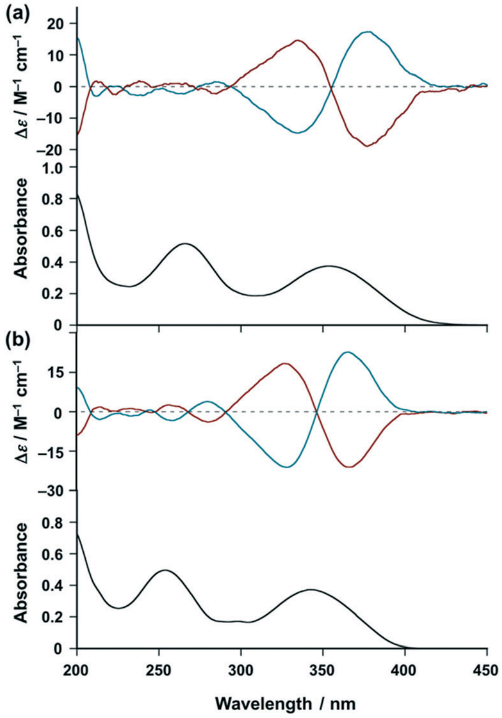

Fig. 3 Top: CD spectra of (a) [(*R*)-iPr-Pybox](Eu^{III})(DK-NO$_2$)$_3$ (red) and [(*S*)-iPr-Pybox](Eu^{III})(DK-NO$_2$)$_3$ (blue), and (b) [(*R*)-iPr-Pybox](Eu^{III})(DK-CN)$_3$ (red) and [(*S*)-iPr-Pybox](Eu^{III})(DK-CN)$_3$ (blue) in acetonitrile at 298 K (concentration: 1.0 × 10^{-5} M). Bottom: Absorption spectrum of (a) [(*S*)-iPr-Pybox](Eu^{III})(DK-NO$_2$)$_3$ and (b) [(*S*)-iPr-Pybox](Eu^{III})(DK-CN)$_3$ (concentration: 1.0 × 10^{-5} M) in acetonitrile at 298 K.

decay curve can be fitted as a sum of three exponential decay components [$I(t) = A_1\exp(-t/\tau_1) + A_2\exp(-t/\tau_2) + A_3\exp(-t/\tau_3)$] with τ_1 = 0.26 ms (11.2%), τ_2 = 0.074 ms (51.8%), and τ_3 = 0.015 ms (37.0%) [Fig. 2a, red solid line], suggesting that three emitting species are present in the solution of [iPr-Pybox](Eu^{III})(DK-NO$_2$)$_3$. As a negative control experiment, [iPr-Pybox](Eu^{III})(DK-CN)$_3$ (reference complex) was synthesized to identify the three emitting species, where the nitro group of the β-diketone was replaced by a cyano group with a lower affinity for Eu^{III}, but with a similar electron withdrawing capacity to the nitro group (Fig. 1). In contrast to the emission decay of [iPr-Pybox](Eu^{III})(DK-NO$_2$)$_3$ (Fig. 2a), the emission of [iPr-Pybox](Eu^{III})(DK-CN)$_3$ obeys a single-exponential decay with a lifetime τ = 0.31 ms (Fig. 2b). The negative results obtained with the reference complex [iPr-Pybox](Eu^{III})(DK-CN)$_3$ suggest that the three emitting species found for [iPr-Pybox](Eu^{III})(DK-NO$_2$)$_3$ are attributed to the chiral Eu^{III} ensemble consisting of several Eu^{III} species, where the pendant nitro group in [iPr-Pybox](Eu^{III})(DK-NO$_2$)$_3$ (monometallic Eu^{III}

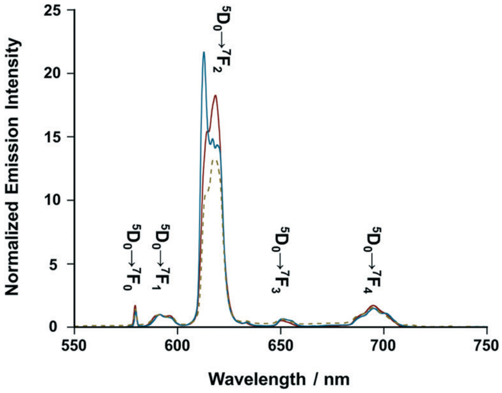

Fig. 4 Emission spectra of [(*S*)-iPr-Pybox](Eu^{III})(DK-NO$_2$)$_3$ (red solid line) and [(*S*)-iPr-Pybox](Eu^{III})(DK-CN)$_3$ (blue solid line) in acetonitrile at 298 K (concentration: 1.0 × 10^{-5} M), and that of [(*S*)-iPr-Pybox](Eu^{III})(DK-NO$_2$)$_3$ in KBr pellet (yellow dashed line), where the emission intensity is normalized at the $^5D_0 \rightarrow {}^7F_1$ transition band. Excitation-wavelength: λ_{ex} = 347 nm.

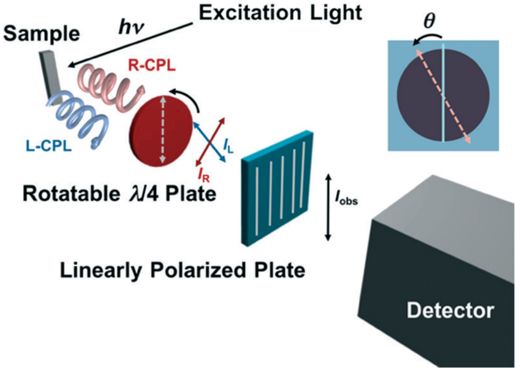

Fig. 5 Schematic illustration of the experimental setup for the determination of g_{lum} values, where "θ" denotes the angle between the rotatable $\lambda/4$ filter and the fixed linearly polarized plate.

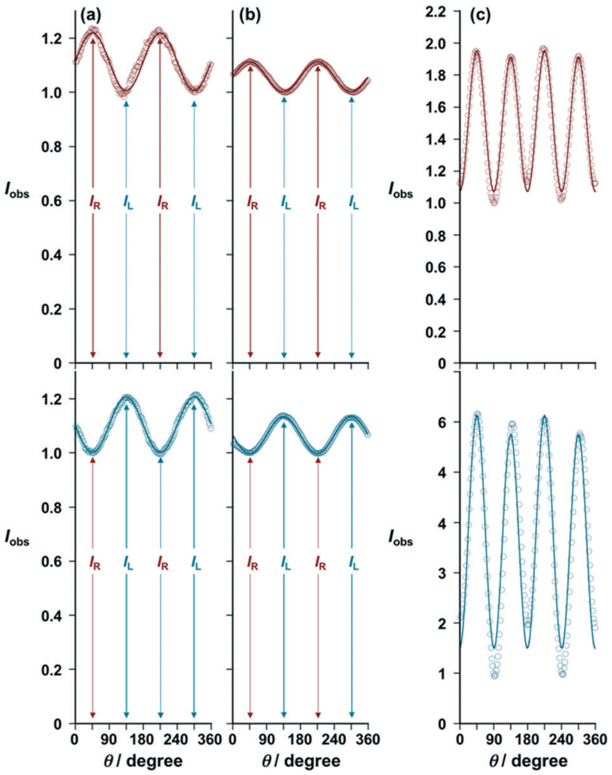

Fig. 6 Plots of emission intensity (I_{obs}) at λ = 594 nm *vs.* the angle (θ) between the rotatable $\lambda/4$ filter and the fixed linearly polarized plate for (a) [(*R*)-iPr-Pybox](Eu^{III})(DK-NO$_2$)$_3$ (red circles) and [(*S*)-iPr-Pybox](Eu^{III})(DK-NO$_2$)$_3$ (blue circles), and (b) [(*R*)-iPr-Pybox](Eu^{III})(DK-CN)$_3$ (red circles) and [(*S*)-iPr-Pybox](Eu^{III})(DK-CN)$_3$ (blue circles) in acetonitrile at 298 K (concentration: 1.0×10^{-5} M), where the intensity was normalized by the minimum value at θ = 45 degrees for the (*S*)-isomers and 135 degrees for the (*R*)-isomers. (c) Those of [(*R*)-iPr-Pybox](Eu^{III})(DK-NO$_2$)$_3$ (red circles) and [(*S*)-iPr-Pybox](Eu^{III})(DK-NO$_2$)$_3$ (blue circles) in the solid state (KBr pellet). Excitation-wavelength: λ_{ex} = 347 nm.

species) coordinates to the Eu^{III} center of another complex (Fig. 1). The lifetime of the longer lifetime component (τ_1 = 0.26 ms (11.2%)) resembles that of the reference monometallic complex [iPr-Pybox](Eu^{III})(DK-CN)$_3$ (τ = 0.31 ms), and hence the longer lifetime component (τ_1 = 0.26 ms) should correspond to the monometallic complex species in the ensemble. Conversely, the shorter lifetime components (τ_2 = 0.074 ms (51.8%) and τ_3 = 0.015 ms (37.0%)) correspond to self-associated complexes (oligomeric Eu^{III} species). The weak coordination between the Eu^{III} ion and the nitro group of DK-NO$_2$ should enhance the non-radiative processes, causing an increase in non-radiative decay rate constants for the self-associated complexes.[14] Then, the Eu^{III} ensemble was investigated by ESI mass spectrometry, where we found mass signals due to the monometallic and dimetallic Eu^{III} species in the ESI mass of [iPr-Pybox](Eu^{III})(DK-NO$_2$)$_3$ in acetonitrile solution, HRMS [ESI-MS (positive)]: *m*/*z* calcd. for $C_{47}H_{38}EuF_9N_6O_{14}Na^+$ [iPr-Pybox](Eu^{III})(DK-NO$_2$)$_3$ + Na)$^+$, 1257.14122; found 1257.14024; *m*/*z* calcd. for $C_{94}H_{76}Eu_2F_{18}N_{12}O_{28}Na^+$ [{[iPr-Pybox](Eu^{III})(DK-NO$_2$)$_3$}$_2$ + Na]$^+$ 2491.30147, found 2491.29268. In addition to these signals, there are several weak mass signals assignable to Eu^{III} complexes containing three Eu^{III} ions, *e.g.*, ESI-MS (positive): *m*/*z* calcd. for $C_{97}H_{63}Eu_3F_{24}N_{11}O_{34}^+$ [[iPr-Pybox](Eu^{III})$_3$(DK-NO$_2$)$_8$]$^+$, 2840.08; found 2840.02. In accordance with these results, we tentatively assigned τ_2 = 0.074 ms to the dimetallic Eu^{III} species ({[iPr-Pybox](Eu^{III})(DK-NO$_2$)$_3$}$_2$) and τ_3 = 0.015 ms to the other oligomeric Eu^{III} species (*e.g.*, trimetallic species). We performed emission lifetime measurement at a higher concentration (1.0×10^{-4} M) of [(*R*)-iPr-Pybox](Eu^{III})(DK-NO$_2$)$_3$ to address this assignment (Fig. S1, ESI†), where the population of the shorter lifetime component (τ_3) due to the oligomeric species increases (from 37.0% to 54.5%) with a concomitant decrease of that of the longer lifetime component due to the monomer species (from 11.2% to 6.0%). This result is consistent with the above assignment. On the other hand, a solid state sample (KBr pellet) of [iPr-Pybox](Eu^{III})(DK-NO$_2$)$_3$ exhibits an emission decay consisting of three exponential components, τ_1 = 0.33 ms (33.4%), τ_2= 0.18 ms (32.1%), and τ_3 = 0.055 ms (34.5%) [Fig. 2c], suggesting that [iPr-Pybox](Eu^{III})(DK-NO$_2$)$_3$ also exists in the ensemble in the solid state.

Chiroptical properties of the chiral Eu^{III} ensemble

With these results in hand, we investigated the chiroptical properties of the chiral Eu^{III} ensemble (*vide infra*). Fig. 3a shows the circular dichroism (CD) spectra of [(*R*)- and (*S*)-iPr-Pybox](Eu^{III})(DK-NO$_2$)$_3$ in acetonitrile (red and blue lines, respectively), where almost complete mirror-image CD signals are obtained with their enantiomer pairs. The chiral Eu^{III} ensemble shows exciton-coupled biphasic (splitting) CD signals at the π–π* transition band (first absorption band) of the β-diketonate moieties (centered at λ = 355 nm),[24] which is due to the induced chiral arrangement of the DK-NO$_2$ ligands around the Eu^{III} center by intra-complex chiral interaction with iPr-Pybox.[21] Similar CD patterns to [(*R*)- and (*S*)-iPr-Pybox](Eu^{III})(DK-NO$_2$)$_3$ are observed for the reference complex

[(*R*)- and (*S*)-iPr-Pybox](Eu^{III})(DK-CN)$_3$ (Fig. 3b). The CD spectrum of the chiral Eu^{III} ensemble (Fig. 3a) is the superposition of the three chiral Eu^{III} complexes (mono-, di-, and the other oligomeric Eu^{III} complexes). Thus, the similar CD patterns between [iPr-Pybox](Eu^{III})(DK-NO$_2$)$_3$ and [iPr-Pybox](Eu^{III})(DK-CN)$_3$ (Fig. 3a and b) indicate that the additional coordination of the –NO$_2$ group to the Eu^{III} center has no significant effect on the exciton-coupling of the DK-NO$_2$ ligands around the Eu^{III} center (intra complex ligand–ligand interactions).

On the other hand, [iPr-Pybox](Eu^{III})(DK-NO$_2$)$_3$ displays sharp emission bands due to the f–f transitions of Eu^{III} ($^5D_0 \rightarrow {}^7F_n$, n = 1–4) in acetonitrile, where each line splits into several lines due to the Stark effect (Fig. 4, red solid line).[25] The spectral shape is different from that of the reference complex [iPr-Pybox](Eu^{III})(DK-CN)$_3$ (Fig. 4, blue solid line) in terms of the Stark splitting pattern of each transition band (except for $^5D_0 \rightarrow {}^7F_0$). Since the emission spectrum of [iPr-Pybox](Eu^{III})(DK-NO$_2$)$_3$ is the superposition of the three emitting species (mono-, di-, and the other oligomeric Eu^{III} complexes), the observed spectral difference indicates a different crystal field environment for the Eu^{III} between the monometallic and the oligomeric Eu^{III} complexes. Conversely, the Stark splitting pattern of [iPr-Pybox](Eu^{III})(DK-NO$_2$)$_3$ in the solid state (Fig. 4, yellow dashed line) roughly agrees with that of the solution sample. This is consistent with the emission lifetime results for [iPr-Pybox](Eu^{III})(DK-NO$_2$)$_3$.

Then, we determined the dissymmetry factors (g_{lum}) of the chiral Eu^{III} ensemble at the $^5D_0 \rightarrow {}^7F_1$ (magnetic dipole) transition band by using the experimental setup for the determination of the g_{lum} values.[14a] Since the magnetic dipole transition satisfies the magnetic-dipole selection rule, $\Delta J = 0, \pm 1$ (except $0 \leftrightarrow 0$), the magnetic dipole transition band often gives particularly large circular polarization.[12] Fig. 5 shows the schematic illustration of the experimental setup used in this study. In this experimental setup, a circularly polarized component (left- and right-CPL) from the sample emission converts to a linearly polarized component after passing through a rotatable $\lambda/4$ filter, which was detected by a photomultiplier tube after passing through a fixed linearly polarized plate (Fig. 5). Thus, the observed emission intensity (I_{obs}) oscillates every 180 degrees of the angle (θ) between the rotatable $\lambda/4$ filter and the fixed linearly polarized plate. The minimal or maximal values appear at θ = 45, 135, 225, and 315 degrees, wherein the values at θ = 45, 225 and 135, 315 degrees correspond to the right- and left-CPL intensity, respectively (I_R and I_L, respectively). With the use of these values, the g_{lum} values were calculated by using the equation, $g_{\text{lum}} = 2(I_L - I_R)/(I_L + I_R)$. As a standard material for the system precision check, we have chosen the cesium tetrakis(3-heptafluoro-butylryl-(+)-camphorato) Eu^{III} complex, Cs$^+$[Eu((+)-hfbc)$_4$]$^-$. So far, Cs$^+$[Eu((+)-hfbc)$_4$]$^-$ shows the highest dissymmetry factor of 1.38 at the $^5D_0 \rightarrow {}^7F_1$ transition band. This system successfully reproduced the literature value of g_{lum} = 1.38 (g_{lum} = 1.41 as determined in this study).[13,14a]

Fig. 6a and b show the measurement data of [(*R*)- and (*S*)-iPr-Pybox](Eu^{III})(DK-NO$_2$)$_3$ and [(*R*)- and (*S*)-iPr-Pybox](Eu^{III})(DK-CN)$_3$ at the $^5D_0 \rightarrow {}^7F_1$ transition (λ = 594 nm) in acetonitrile solution, respectively. Almost complete mirror-image oscillation patterns are obtained with their enantiomer pairs (Fig. 6a and b, red: (*R*)-isomers; blue: (*S*)-isomers). The oscillation patterns (every 180 degrees) are well reproduced by the simulation curves provided by eqn (1) [θ in radians] with I_L/I_R = 0.82 for [(*R*)-iPr-Pybox](Eu^{III})(DK-NO$_2$)$_3$ (Fig. 6a, red line), I_L/I_R = 1.21 for [(*S*)-iPr-Pybox](Eu^{III})(DK-NO$_2$)$_3$ (Fig. 6a, blue line), I_L/I_R = 0.90 for [(*R*)-iPr-Pybox](Eu^{III})(DK-CN)$_3$ (Fig. 6b, red line), and I_L/I_R = 1.13 for [(*S*)-iPr-Pybox](Eu^{III})(DK-CN)$_3$ (Fig. 6b, blue line). The obtained chiroptical parameters are summarized in Table 1, in which the chiral Eu^{III} ensemble of [iPr-Pybox](Eu^{III})(DK-NO$_2$)$_3$ exhibits a higher dissymmetry factor ($|g_{\text{lum}}|$ = 0.19) than that of the monometallic complex of [iPr-Pybox](Eu^{III})(DK-CN)$_3$ ($|g_{\text{lum}}|$ = 0.11–0.13). The monometallic complex (n = 1) in the chiral Eu^{III} ensemble {[(*R*)- or (*S*)-iPr-Pybox](Eu^{III})(DK-NO$_2$)$_3$}$_n$ should possess a similar luminescence dissymmetry factor (g_{lum1}) to that of the reference monometallic complex [iPr-Pybox](Eu^{III})(DK-CN)$_3$, therefore the large difference in the luminescence dissymmetry factor is primarily due to the contribution of the higher degree of circular polarization in luminescence of the dimetallic and the other oligomeric Eu^{III} species (g_{lum2} and g_{lum3}, respectively). In such a case, the observed (overall) luminescence dissymmetry factor (g_{overall}) can be expressed using eqn (2), where Φ_{total} denotes the total emission quantum yield of the chiral Eu^{III} ensemble ($\Phi_{\text{em1}} + \Phi_{\text{em2}} + \Phi_{\text{em3}}$). Φ_{em1}, Φ_{em2}, and Φ_{em3} represent the emission quantum yields of the mono-, di-, and the other oligomeric Eu^{III} species, respectively. The $\Phi_{\text{em1}}/\Phi_{\text{total}}$, $\Phi_{\text{em2}}/\Phi_{\text{total}}$, and $\Phi_{\text{em3}}/\Phi_{\text{total}}$ terms can be calculated using eqn (3)–(5) with the emission lifetime parameters (A_{1-3} and τ_{1-3}). The $\Phi_{\text{em1-3}}/\Phi_{\text{total}}$ values were determined to be $\Phi_{\text{em1}}/\Phi_{\text{total}}$ = 0.39, $\Phi_{\text{em2}}/\Phi_{\text{total}}$ = 0.53, and $\Phi_{\text{em3}}/\Phi_{\text{total}}$ = 0.077. Then, the overall luminescence dissymmetry factor (g_{overall}) can be expressed using eqn (6), where $\Phi_{\text{em3}}/\Phi_{\text{total}}$ could be negligible compared to $\Phi_{\text{em1}}/\Phi_{\text{total}}$ and $\Phi_{\text{em2}}/\Phi_{\text{total}}$ mostly due to the low emission efficiency ($\tau_3 \ll \tau_1, \tau_2$). Consequently, $|g_{\text{lum2}}|$ = 0.27 would be derived when assuming that the monometallic complex in the chiral Eu^{III} ensemble has the same luminescence dissymmetry factor (g_{lum1}) as that of the reference monometallic complex (g_{lum} = 0.13). The larger luminescence dissymmetry factor ($|g_{\text{lum2}}|$ = 0.27) of the dimetallic Eu^{III} complex may be due to the additional coordination of the –NO$_2$ group to the Eu^{III} center, causing a higher degree of dissymmetry in the coordination geometry (crystal field).[21]

Table 1 Chiroptical parameters (I_L/I_R and g_{lum}) of [(*R*)- and (*S*)-iPr-Pybox](Eu^{III})(DK-NO$_2$)$_3$ and [(*R*)- and (*S*)-iPr-Pybox](Eu^{III})(DK-CN)$_3$ in acetonitrile at the $^5D_0 \rightarrow {}^7F_1$ transition

	I_L/I_R	g_{lum}
[(*R*)-iPr-Pybox](Eu^{III})(DK-NO$_2$)$_3$	0.82	−0.19
[(*S*)-iPr-Pybox](Eu^{III})(DK-NO$_2$)$_3$	1.21	0.19
[(*R*)-iPr-Pybox](Eu^{III})(DK-CN)$_3$	0.90	−0.11
[(*S*)-iPr-Pybox](Eu^{III})(DK-CN)$_3$	1.13	0.13

$$I_{\mathrm{obs}} = I_{\mathrm{L}}\cos^2(\theta + \pi/4) + I_{\mathrm{R}}\sin^2(\theta + \pi/4) \tag{1}$$

$$g_{\mathrm{overall}} = (g_{\mathrm{lum1}}\Phi_{\mathrm{em1}} + g_{\mathrm{lum2}}\Phi_{\mathrm{em2}} + g_{\mathrm{lum3}}\Phi_{\mathrm{em3}})/\Phi_{\mathrm{total}} \tag{2}$$

$$\Phi_{\mathrm{em1}}/\Phi_{\mathrm{total}} = (A_1\tau_1)/(A_1\tau_1 + A_2\tau_2 + A_3\tau_3) \tag{3}$$

$$\Phi_{\mathrm{em2}}/\Phi_{\mathrm{total}} = (A_2\tau_2)/(A_1\tau_1 + A_2\tau_2 + A_3\tau_3) \tag{4}$$

$$\Phi_{\mathrm{em3}}/\Phi_{\mathrm{total}} = (A_3\tau_3)/(A_1\tau_1 + A_2\tau_2 + A_3\tau_3) \tag{5}$$

$$g_{\mathrm{overall}} = 0.39g_{\mathrm{lum1}} + 0.53g_{\mathrm{lum2}} + 0.077g_{\mathrm{lum3}} \tag{6}$$

Fig. 6c shows the measurement data of [(*R*)- and (*S*)-iPr-Pybox](Eu$^{\mathrm{III}}$)(DK-NO$_2$)$_3$ in the solid state (KBr pellet) at the ^{5}D$_0$ → ^{7}F$_1$ transition (λ = 594 nm). The I_{obs} value oscillates every 90 degrees of the angle (θ) between the rotatable $\lambda/4$ filter and the fixed linearly polarized plate (minimal values at 0, 90, 180, 270, and 360 degrees; maximum values at 45, 135, 225, and 315), where no mirror-image oscillation patterns can be obtained with their enantiomer pairs [Fig. 6c, red: (*R*)-isomer; blue: (*S*)-isomer]. This shows a sharp contrast to the solution samples (Fig. 6a and b). The oscillation at every 90 degrees corresponds to the linearly polarized component from the sample emission, suggesting that the luminescence from [iPr-Pybox](Eu$^{\mathrm{III}}$)(DK-NO$_2$)$_3$ in the solid state (KBr pellet) contains a large linearly polarized component. The accurate dissymmetry factor could not be obtained from these measurement data due to the large contribution of the linearly polarized component. Conversely, there is no appreciable linearly polarized component in the solution samples, where the observed emission intensity (I_{obs}) oscillates every 180 degrees (Fig. 6a and b). The presented measuring system is typically suitable for accurate determination of the luminescence dissymmetry factor of lanthanide complexes in solutions.[26]

Conclusions

In conclusion, we have demonstrated how to evaluate the luminescence dissymmetry factor in an ensemble consisting of several Eu$^{\mathrm{III}}$ complex species exhibiting different chiroptical properties. The chiral Eu$^{\mathrm{III}}$ complex [(*R*)- or (*S*)-iPr-Pybox](Eu$^{\mathrm{III}}$)(DK-NO$_2$)$_3$ spontaneously forms the oligomeric Eu$^{\mathrm{III}}$ species, {[iPr-Pybox](Eu$^{\mathrm{III}}$)(DK-NO$_2$)$_3$}$_n$, in acetonitrile, where the pendant nitro group in [iPr-Pybox](Eu$^{\mathrm{III}}$)(DK-NO$_2$)$_3$ (monometallic Eu$^{\mathrm{III}}$ species) coordinates to the Eu$^{\mathrm{III}}$ center of another complex. Consequently, [iPr-Pybox](Eu$^{\mathrm{III}}$)(DK-NO$_2$)$_3$ exists in an ensemble consisting of three chiral Eu$^{\mathrm{III}}$ complex species. Among them, the dimetallic chiral Eu$^{\mathrm{III}}$ complex shows a larger dissymmetry factor ($|g_{\mathrm{lum2}}|$ = 0.27) than that of the monometallic Eu$^{\mathrm{III}}$ complex, resulting in an increase of the overall luminescence dissymmetry factor of the chiral Eu$^{\mathrm{III}}$ ensemble ($|g_{\mathrm{lum}}|$ = 0.19). The demonstrated methodology for the evaluation of circularly polarized luminescence of the chiral Eu$^{\mathrm{III}}$ ensemble will open up new opportunities for developing supramolecular chiral lanthanide systems.

Conflicts of interest

There are no conflicts to declare.

Acknowledgements

This work was partly supported by JST-PRESTO "Molecular technology and creation of new functions" (14530027), a Grant-in-Aid for Scientific Research (C) (JP26410094) from the Ministry of Education, Culture, Sports, Science and Technology, Japan and also JSPS KAKENHI Grant Number JP17H05386 (Coordination Asymmetry).

Notes and references

1 (*a*) D. L. Andrews, in *Photonics, Fundamental of Photonics and Physics*, Wiley, Hoboken, 2015, vol. 1; (*b*) *Comprehensive Chiroptical Spectroscopy Instrumentation, Methodologies, and Theoretical Simulations*, ed. N. Berova, P. L. Polavarapu, K. Nakanishi and R. W. Woody, Wiley, Hoboken, 2012, vol. 1.

2 Y. J. Zhang, T. Oka, R. Suzuki, J. T. Ye and Y. Iwasa, *Science*, 2014, **344**, 725.

3 F. Zinna, U. Giovanella and L. Di Bari, *Adv. Mater.*, 2015, **27**, 1791.

4 J. P. Riehl and G. Muller, in *Handbook on the Physics and Chemistry of Rare Earths*, ed. K. A. Gschneidner Jr., J.-C. G. Bünzli and V. K. Pecharsky, North Holland Publishing Company, Amsterdam, 2005, ch. 220, vol. 34, p. 289.

5 (*a*) R. Carr, N. H. Evans and D. Parker, *Chem. Soc. Rev.*, 2012, **41**, 7673; (*b*) C. M. G. dos Santos, A. J. Harte, S. J. Quinn and T. Gunnlaugsson, *Coord. Chem. Rev.*, 2008, **252**, 2512; (*c*) J.-C. G. Bünzli and C. Piguet, *Chem. Soc. Rev.*, 2005, **34**, 1048.

6 (*a*) E. G. Moore, A. P. S. Samuel and K. N. Raymond, *Acc. Chem. Res.*, 2009, **42**, 542; (*b*) G.-L. Law, C. M. Andolina, J. Xu, V. Luu, P. X. Rutkowski, G. Muller, D. K. Shuh, J. K. Gibson and K. N. Raymond, *J. Am. Chem. Soc.*, 2012, **134**, 15545.

7 (*a*) M. Cantuel, G. Bernardinelli, G. Muller, J. P. Riehl and C. Piguet, *Inorg. Chem.*, 2004, **43**, 1840; (*b*) G. Muller, J. P. Riehl, K. J. Schenk, G. Hopfgartner, C. Piguet and J.-C. G. Bünzli, *Eur. J. Inorg. Chem.*, 2002, 3101; (*c*) G. Muller, B. Schmidt, J. Jiricek, G. Hopfgartner, J. P. Riehl, J.-C. G. Bünzli and C. Piguet, *J. Chem. Soc., Dalton Trans.*, 2001, 2655; (*d*) S. D. Bonsall, M. Houcheime, D. A. Straus and G. Muller, *Chem. Commun.*, 2007, 3676.

8 (*a*) O. Mamula, M. Lama, S. G. Telfer, A. Nakamura, R. Kuroda, H. Stoeckli-Evans and R. Scopelitti, *Angew. Chem., Int. Ed.*, 2005, **44**, 2527; (*b*) M. Lama, O. Mamula, G. S. Kottas, F. Rizzo, L. De Cola, A. Nakamura, R. Kuroda and H. Stoeckli-Evans, *Chem. – Eur. J.*, 2007, **13**, 7358.

9 (*a*) A. de Bettencourt-Dias, P. S. Barber and S. Bauer, *J. Am. Chem. Soc.*, 2012, **134**, 6987; (*b*) A. de Bettencourt-Dias, S. Viswanathan and A. Rollett, *J. Am. Chem. Soc.*, 2007, **129**, 15436; (*c*) S. Chorazy, K. Nakabayashi, M. Arczynski, R. Pełka, S.-I. Ohkoshi and B. Sieklucka, *Chem. – Eur. J.*, 2014, **20**, 7144; (*d*) K. Matsumoto, K. Suzuki, T. Tsukuda and T. Tsubomura, *Inorg. Chem.*, 2010, **49**, 4717.

10 (*a*) J. I. Bruce, R. S. Dickins, L. J. Govenlock, T. Gunnlaugsson, S. Lopinski, M. P. Lowe, D. Parker, R. D. Peacock, J. J. B. Perry, S. Aime and M. Botta, *J. Am. Chem. Soc.*, 2000, **122**, 9674; (*b*) J. P. Leonard, P. Jensen, T. McCabe, J. E. O'Brien, R. D. Peacock, P. E. Kruger and T. Gunnlaugsson, *J. Am. Chem. Soc.*, 2007, **129**, 10986.

11 (*a*) J. Gregoliński and J. Lisowski, *Angew. Chem., Int. Ed.*, 2006, **45**, 6122; (*b*) J. Gregoliński, P. Starynowicz, K. T. Hua, J. L. Lunkley, G. Muller and J. Lisowski, *J. Am. Chem. Soc.*, 2008, **130**, 17761.

12 F. S. Richardson, *Inorg. Chem.*, 1980, **19**, 2806.

13 J. L. Lunkley, D. Shirotani, K. Yamanari, S. Kaizaki and G. Muller, *J. Am. Chem. Soc.*, 2008, **130**, 13814.

14 (*a*) J. Kumar, B. Marydasan, T. Nakashima, T. Kawai and J. Yuasa, *Chem. Commun.*, 2016, **52**, 9885; (*b*) J. Yuasa, H. Ueno and T. Kawai, *Chem. – Eur. J.*, 2014, **20**, 8621.

15 C.-T. Yeung, W. T. K. Chan, S.-C. Yan, K.-L. Yu, K.-H. Yim, W.-T. Wong and G.-L. Law, *Chem. Commun.*, 2015, **51**, 592.

16 (*a*) K. S. Jeong, Y. S. Kim, Y. J. Kim, E. Lee, J. H. Yoon, W. H. Park, Y. W. Park, S.-J. Jeon, Z. H. Kim, J. Kim and N. Jeong, *Angew. Chem., Int. Ed.*, 2006, **45**, 8134; (*b*) X.-J. Kong, Y. Wu, L.-S. Long, L.-S. Zheng and Z. Zheng, *J. Am. Chem. Soc.*, 2009, **131**, 6918.

17 (*a*) G. Bozoklu, C. Marchal, C. Gateau, J. Pécaut, D. Imbert and M. Mazzanti, *Chem. – Eur. J.*, 2010, **16**, 6159; (*b*) G. Bozoklu, C. Gateau, D. Imbert, J. Pécaut, K. Robeyns, Y. Filinchuk, F. Memon, G. Muller and M. Mazzanti, *J. Am. Chem. Soc.*, 2012, **134**, 8372; (*c*) X.-L. Tang, W.-H. Wang, W. Dou, J. Jiang, W.-S. Liu, W.-W. Qin, G.-L. Zhang, H.-R. Zhang, K.-B. Yu and L.-M. Zheng, *Angew. Chem., Int. Ed.*, 2009, **48**, 3499.

18 (*a*) J. Gregoliński, P. Starynowicz, K. T. Hua, J. L. Lunkley, G. Muller and J. Lisowski, *J. Am. Chem. Soc.*, 2008, **130**, 17761; (*b*) J. Lisowski, *Inorg. Chem.*, 2011, **50**, 5567.

19 In this context, we have extensively developed self-assembly in an ensemble system, see: (*a*) T. Ogawa, J. Yuasa and T. Kawai, *Angew. Chem., Int. Ed.*, 2010, **49**, 5110; (*b*) J. Yuasa, A. Mitsui and T. Kawai, *Chem. Commun.*, 2011, **47**, 5807; (*c*) N. Inukai, T. Kawai and J. Yuasa, *Chem. Commun.*, 2011, **47**, 9128; (*d*) N. Inukai, T. Kawai and J. Yuasa, *Chem. – Eur. J.*, 2013, **19**, 5938; (*e*) N. Inukai, T. Kawai and J. Yuasa, *Chem. – Eur. J.*, 2014, **20**, 15159; (*f*) Y. Imai, T. Kawai and J. Yuasa, *J. Phys. Chem. A*, 2016, **120**, 4131; (*g*) Y. Imai, T. Kawai and J. Yuasa, *Chem. Commun.*, 2015, **51**, 10103.

20 M. Hasegawa, H. Ohtsu, D. Kodama, T. Kasai, S. Sakurai, A. Ishiia and K. Suzuki, *New J. Chem.*, 2014, **38**, 1225.

21 J. Yuasa, T. Ohno, K. Miyata, H. Tsumatori, Y. Hasegawa and T. Kawai, *J. Am. Chem. Soc.*, 2011, **133**, 9892.

22 J. C. Sloop, P. D. Boyle, A. W. Fountain, W. F. Pearman and J. A. Swann, *Eur. J. Org. Chem.*, 2011, 936.

23 Y. Hasegawa, S. Tsuruoka, T. Yoshida, H. Kawai and T. Kawai, *J. Phys. Chem. A*, 2008, **112**, 803.

24 S. G. Telfer, N. Tajima and R. Kuroda, *J. Am. Chem. Soc.*, 2004, **126**, 1408.

25 (*a*) J. Yuasa, R. Mukai, Y. Hasegawa and T. Kawai, *Chem. Commun.*, 2014, **50**, 7937; (*b*) J. Yuasa, T. Ohno, H. Tsumatori, R. Shiba, H. Kamikubo, M. Kataoka, Y. Hasegawa and T. Kawai, *Chem. Commun.*, 2013, **49**, 4604; (*c*) J. Yuasa, T. Nakagawa, Y. Kita, A. Kaito and T. Kawai, *Chem. Commun.*, 2017, **53**, 6748.

26 The lower detection limit of the *g*-value by this method should be 0.01.